Modeling off-resonant nonlinear-optical cascading in mesoscopic thin films and guest-host molecular systems

Nathan J. Dawson, James H. Andrews, and Michael Crescimanno
Department of Physics and Astronomy, Youngstown State University, Youngstown, OH 44555[*]

We develop a model for off-resonant microscopic cascading of scalar polarizabilities using a self-consistent field approach, and use it to study the effects of boundaries on mesoscopic systems of nonlinear polarizable atoms and molecules. We find that higher-ordered susceptibilities can be enhanced by increasing the surface-to-volume ratio through reducing the distance between boundaries perpendicular to the linear polarization. We also show lattice scaling effects on the effective nonlinear refractive indices for Gaussian beams, and illustrate finite size effects on dipole field distributions in films subject to long-wavelength propagating fields. We derive simplified expressions for the microscopic cascading of the nonlinear optical response in guest-host systems.

I. INTRODUCTION

It is well-known that cascaded nonlinear optical interactions and local field effects at the molecular level can enhance higher-order nonlinear optical susceptibilities.[1–4] Dolgaleva, *et al.*, showed that local-field corrections predict trends in the nonlinear susceptibilities as functions of concentration in a bulk material.[5–8] Earlier studies focused on a tensor formalism to describe correlated cascading effects in bulk materials,[1] while others focused on cascading between coupled molecules only.[4, 9] Mesoscale nonlinear optical effects, however, have not been well investigated, and give new insights into enhancing the nonlinear susceptibility that are not present in a bulk approximation.[10] Here, we use the self-consistent field approach to cascading (Bloembergen's method [11]) to approximate the local field factors and the cascading contribution in mesoscopic systems.

We compute the effective (hyper)polarizabilities and susceptibilities with respect to the applied field by an iterative update method to approximate a finite ensemble of polarizable molecules. After describing the method in Section II, we apply it in Section III to bounded and strained tetragonal systems. The dipolar field at each molecule from all other molecules is shown for different film thicknesses, where the dipoles are induced by a linear polarized Gaussian beam. Then, as an application to a real system, we find that the relationship between the cascading contribution of hexagonal close-packed and honeycomb structured monolayers of the molecule C_{60} can be understood by the fill factor and concentration. Finally, in Section IV we approximate the effective second hyperpolarizability of a mesoscale guest-host system in which a nonlinear dopant has been randomly distributed in a discretized linear matrix, providing an example of matrix-enhanced dye polarizability.

[*] Corresponding author: dawsphys@hotmail.com

II. THEORY

A. Self-consistent approach

When point molecule j is polarized by an electric field, it becomes a dipole, causing molecule $i \neq j$ to experience a corresponding dipole field

$$\boldsymbol{E}_{i,j} = \frac{3\left(\hat{r}_i - \hat{r}_j\right)\left[\boldsymbol{p}_j \cdot \left(\hat{r}_i - \hat{r}_j\right)\right] - \boldsymbol{p}_j}{\left|\boldsymbol{r}_i - \boldsymbol{r}_j\right|^3}, \tag{1}$$

where $\boldsymbol{p}_j$ is the dipole moment of molecule j, $|\boldsymbol{r}_i - \boldsymbol{r}_j|$ is the molecular separation, and $\hat{r}$ is a unit vector.

We introduce the geometric tensor $g_{\alpha\beta\,|i,j}$ in a cartesian coordinate system, relating $\boldsymbol{p}_j$ to $\boldsymbol{E}_{i,j}$ from Eq. (1),

$$g_{\alpha\beta\,|i,j} = \left(3[(\hat{r}_i - \hat{r}_j)\cdot\hat{\alpha}][(\hat{r}_i - \hat{r}_j)\cdot\hat{\beta}] - \boldsymbol{\delta}_{\alpha\beta}\right)\frac{v_c}{\left|\boldsymbol{r}_i - \boldsymbol{r}_j\right|^3}, \tag{2}$$

where the Greek subscripts represent the spatial cartesian components and $\boldsymbol{\delta}_{\alpha\beta}$ is the Kronecker delta. Here, we have introduced a characteristic volume, v_c, which makes the geometric tensor dimensionless.

When the total electric field at molecule i is sufficiently small, its dipole moment can be approximated as a power series,

$$\begin{aligned} p_{\alpha\,|i} = {} & k^{(0)}_{\alpha\,|i} + k^{(1)}_{\alpha\beta\,|i} E_{\beta\,|i} + k^{(2)}_{\alpha\beta\mu\,|i} E_{\beta\,|i} E_{\mu\,|i} \\ & + k^{(3)}_{\alpha\beta\mu\nu\,|i} E_{\beta\,|i} E_{\mu\,|i} E_{\nu\,|i} + \cdots, \end{aligned} \tag{3}$$

where $k^{(n)}_i$ is the nth-order polarizability of the ith molecule.

In a system of N molecules, the total electric field is the vector sum of the applied field and the dipole fields due to all other molecules (higher-order multipole moments are ignored and we use a dipole approximation). Thus,

$$E_{\alpha\,|i} = E^a_{\alpha\,|i} + \sum_{j\neq i}^{N-1} E^d_{\alpha\,|i,j}, \tag{4}$$

where $E^a_{\alpha\,|i}$ is the α component of the applied field at the ith molecule and $E^d_{\alpha\,|i,j}$ is the α component of the

dipole field at the ith molecule from the jth molecule. It is common to write the linear and nonlinear responses in terms of the macroscopic field. Due to the microscopic focus of this paper, we have defined the effective polarizability and susceptibility in terms of the applied field, $\boldsymbol{E}^a$, where the depolarization field [12] and self-field [13] are included in the summation of all other dipole contributions to the electric field.[10] Because of Eq. (2), the dipole field can then be rewritten as

$$E^d_{\alpha\,|i,j} = g_{\alpha\beta\,|i,j}\frac{p_{\beta\,|j}}{v_c}. \tag{5}$$

Because of the computational approach we use, it is natural to scale all $\left|\boldsymbol{p}_j\right|$ to $|\boldsymbol{p}_i|$ defining,

$$g^{(N-1)}_{\alpha\beta\,|i} = \sum_{j\neq i}^{N-1} g_{\alpha\beta\,|i,j}\mathcal{P}_{\beta\,|i,j}, \tag{6}$$

where

$$\mathcal{P}_{\alpha\,|i,j} = \frac{p_{\alpha\,|j}}{p_{\alpha\,|i}}. \tag{7}$$

The factor $g^{(N-1)}_{\alpha\beta\,|i}$ depends on the particular map of the *a priori* molecular polarizations. A brute force approach would be to solve the set of polarization equations for every interacting molecule in the system. A simpler approach would be to approximate the value of $\mathcal{P}_{\alpha\,|i,j}$ with an iterative method. Choosing the latter approach, we solve for $p^{[1]}_{\alpha\,|i}$ in the equation

$$\begin{aligned} p^{[1]}_{\alpha\,|i} = {} & k^{(0)}_{\alpha\,|i} + k^{(1)}_{\alpha\beta\,|i}\left(E^a_{\beta\,|i} + \sum_{j\neq i}^{N-1} g_{\beta\gamma\,|i,j}\mathcal{P}^{[0]}_{\gamma\,|i,j}\frac{p^{[1]}_{\gamma\,|i}}{v_c}\right) \\ & + k^{(2)}_{\alpha\beta\mu\,|i}\left(E^a_{\beta\,|i} + \sum_{j\neq i}^{N-1} g_{\beta\gamma\,|i,j}\mathcal{P}^{[0]}_{\gamma\,|i,j}\frac{p^{[1]}_{\gamma\,|i}}{v_c}\right) \\ & \times\left(E^a_{\mu\,|i} + \sum_{j\neq i}^{N-1} g_{\mu\gamma\,|i,j}\mathcal{P}^{[0]}_{\gamma\,|i,j}\frac{p^{[1]}_{\gamma\,|i}}{v_c}\right) + \cdots, \end{aligned} \tag{8}$$

where

$$\mathcal{P}^{[0]}_{\alpha\,|i,j} = \frac{p^{[0]}_{\alpha\,|j}}{p^{[0]}_{\alpha\,|i}} \tag{9}$$

and

$$p^{[0]}_{\alpha\,|i} = k^{(0)}_{\alpha\,|i} + k^{(1)}_{\alpha\beta\,|i}E^a_{\beta\,|i} + k^{(2)}_{\alpha\beta\mu\,|i}E^a_{\beta\,|i}E^a_{\mu\,|i} + \cdots. \tag{10}$$

Then through an iterative method we solve for $p^{[n]}_{\alpha\,|i}$ via the previously evaluated $\mathcal{P}^{[n-1]}_{\alpha\,|i,j}$. The Appendix discusses the iterative process for higher-order corrections when a single iteration is not a sufficient approximation of $\mathcal{P}_{\alpha\,|i,j}$.

Far from the strongly coupled regime, we approximate the interactions using only the first-order iterative correction. Then, we define

$$f^{(N-1)}_{\alpha\beta\,|i} = \sum_{j\neq i}^{N-1} g_{\alpha\beta\,|i,j}\mathcal{P}^{[0]}_{\beta\,|i,j}, \tag{11}$$

where, to zeroth iterative order, $p^{[0]}$ is the dipole moment of a molecule subject to only the applied field. Note that in this weakly coupled regime $f^{(N-1)}_{\alpha\beta\,|i} \approx g^{(N-1)}_{\alpha\beta\,|i}$ because the intermolecular responses are much less than every molecule's response to the slowly varying applied field, *i.e.*, when $k^{(1)}/r^3 \ll 1$. In addition, Eq. (11) presupposes $E^a_i \neq 0$.

For dipole field distributions, $\mathcal{P}^{[0]}_{\alpha\,|i,j}$ can be approximated by E^a_j/E^a_i when $k^{(1)}E^a \gg k^{(n)}\left(E^a\right)^n$ for $n > 1$; otherwise, the values of $k^{(n)}_{\alpha\beta\mu\nu\cdots}$ must be known to find a value for $f^{(N-1)}_{\alpha\beta\,|i}$. We use this approximation to generate dipole field maps, illustrated in Section III B. Again, for strongly interacting systems, we stress that higher-order corrections to the self-consistent equation described in the Appendix may be necessary for a more accurate approximation of $g^{(N-1)}_{\alpha\beta\,|i}$.

Assuming that the second-order correction to the dipole field contribution is small, substituting Eq. (11) into Eq. (8) gives

$$\begin{aligned} p_{\alpha\,|i} \approx {} & k^{(0)}_{\alpha\,|i} + k^{(1)}_{\alpha\beta\,|i}\left(E^a_{\beta\,|i} + f^{(N-1)}_{\beta\mu\,|i}\frac{p_{\mu\,|i}}{v_c}\right) \\ & + k^{(2)}_{\alpha\beta\mu\,|i}\left(E^a_{\beta\,|i} + f^{(N-1)}_{\beta\gamma\,|i}\frac{p_{\gamma\,|i}}{v_c}\right)\left(E^a_{\mu\,|i} + f^{(N-1)}_{\mu\nu\,|i}\frac{p_{\nu\,|i}}{v_c}\right) \\ & + \cdots. \end{aligned} \tag{12}$$

Using Eq. (12), we solve for the effective (hyper)polarizabilities, using

$$k^{(n)}_{\mathrm{eff},\alpha\beta\mu\nu\cdots\,|i} = \frac{1}{n!}\frac{\partial^n p_{\alpha\,|i}}{\partial E^a_{\alpha\,|i}\partial E^a_{\beta\,|i}\partial E^a_{\mu\,|i}\partial E^a_{\nu\,|i}\cdots}\bigg|_{\boldsymbol{E}^a=0}. \tag{13}$$

B. Application to one-dimensional polarizable molecules

We eliminate the possibility of higher-order terms appearing in the lower-order effective (hyper)polarizabilities by assuming molecules with negligible permanent dipoles. This approximation still permits molecules having any higher-order response.[14] We assume that the only relevant tensor component is in the direction of the applied field. Also, we assume a lattice model, where molecules are located only at lattice points.[15–17] Note that a lattice model is not necessary, but this approach allows for fast computation time when simulating the dipolar field contributions in the sections below.

Taking the applied field to be unidirectional and parallel to the z-axis, we reduce the tensor $f^{(N-1)}_{\alpha\beta\,|i}$ to a vector $f^{(N-1)}_{\alpha z\,|i}$. Because we are assuming a lattice model, we take the characteristic volume v_c to be the volume of a unit cell, $v = |\boldsymbol{a}\cdot(\boldsymbol{b}\times\boldsymbol{c})|$, where $\boldsymbol{a}$, $\boldsymbol{b}$, and $\boldsymbol{c}$ are the lattice vectors. Thus, the sum of the field contributions of all other molecules becomes

$$\sum_{j\neq i}^{N-1} E^d_{\alpha\,|i,j} = f^{(N-1)}_{\alpha z\,|i}\frac{p_{z\,|i}}{v}. \tag{14}$$

Note that the dimensionless geometric vector is scaled to the ith dipole that is induced by the applied field. Under these approximations and simplifications, we can now write the simplified equation for the induced dipole moment in the z-direction,

$$p_{z\,|i} = \sum_{n=1} k^{(n)}_{zz\cdots}\left(E^a_i + f^{(N-1)}_{zz\,|i}\frac{p_{z\,|i}}{v}\right)^n, \tag{15}$$

where $\boldsymbol{E}^a = E^a\hat{z}$.

Again, we emphasize that, at this point, we assume that the dipoles are only polarized in the direction of the applied field and that the contributions from all (hyper)polarizability tensor components other than $k^{(n)}_{zzz\cdots}$ are negligible. Although this model may oversimplify some scenarios that require the consideration of molecular orientation (see Section IV), it allows for a single self-consistent equation that evaluates the effective scalar (hyper)polarizabilities with respect to the applied field at each molecular site. Solving Eq. (15) self-consistently for the dipole moment and substituting it into

$$k^{(n)}_{\text{eff},i} = \frac{1}{n!}\frac{\partial^n p_i}{\partial\left(E^a_i\right)^n}\bigg|_{E^a_i=0}, \tag{16}$$

gives the effective scalar (hyper)polarizabilities used to evaluate the susceptibilities in terms of the applied field. For example, a system of linearly polarizable molecules with no permanent dipole moment has an effective linear polarizability written as

$$k^{(1)}_{\text{eff},i} = L_i k^{(1)}, \tag{17}$$

where the local field factor, L_i, at the ith molecule's location is given by

$$L_i = \left(1 - f^{(N-1)}_{zz\,|i}\frac{k^{(1)}}{v}\right)^{-1}. \tag{18}$$

For a convergent solution everywhere, $k^{(1)}f^{(N-1)}_{zz\,|i} < v$ for all i molecules, otherwise the local field factor diverges.[9, 18] The average linear susceptibility is then written as

$$\left\langle\chi^{(1)}\right\rangle = \frac{1}{Nv}\sum_{i=1}^{N} k^{(1)}_{\text{eff},i}. \tag{19}$$

Here, χ is defined in terms of the applied field. Thus, Eq. (18) is analogous, but not equal, to the Lorentz-Lorenz local field factor.

C. First-order corrections to nonlinear microscopic cascading

Cascading lower-order nonlinearities to give higher-order nonlinear responses has been well understood and is inherent to the power series approximation of nonlinear optics.[1, 8, 19, 20] The effective (hyper)polarizabilities are a combination of the highest-order response and cascaded lower-order responses. When near resonance, one must be careful to account for the imaginary (non-degenerate frequency mixing, absorption, etc.) and real (linear and nonlinear indices) components of the (hyper)polarizabilities. All tensor components are approximately real in the far off-resonant (below resonance) case to which we limit ourselves.

Taking into account only the largest contributing tensor component of the real molecular responses (the components purely in the direction of the applied field), and under the approximations in Section II B, the first through sixth effective hyperpolarizabilities are formally given as

$$k^{(2)}_{\text{eff},i} = L_i^3 k^{(2)}, \tag{20}$$

$$k^{(3)}_{\text{eff},i} = L_i^4 k^{(3)} + 2L_i^5 F_i\left(k^{(2)}\right)^2, \tag{21}$$

$$k^{(4)}_{\text{eff},i} = L_i^5 k^{(4)} + 5L_i^6 F_i k^{(2)} k^{(3)} + 5L_i^7 F_i^2\left(k^{(2)}\right)^3, \tag{22}$$

$$\begin{aligned} k^{(5)}_{\text{eff},i} = {} & L_i^6 k^{(5)} + 3L_i^7 F_i\left[\left(k^{(3)}\right)^2 + 2k^{(2)}k^{(4)}\right] \\ & + 21L_i^8 F_i^2\left(k^{(2)}\right)^2 k^{(3)} + 14L_i^9 F_i^3\left(k^{(2)}\right)^4, \end{aligned} \tag{23}$$

$$\begin{aligned} k^{(6)}_{\text{eff},i} = {} & L_i^7 k^{(6)} + 7L_i^8 F_i\left[k^{(3)}k^{(4)} + k^{(2)}k^{(5)}\right] \\ & + 28L_i^9 F_i^2 k^{(2)}\left[\left(k^{(3)}\right)^2 + k^{(2)}k^{(4)}\right] \\ & + 84L_i^{10} F_i^3\left(k^{(2)}\right)^3 k^{(3)} + 42L_i^{11} F_i^4\left(k^{(2)}\right)^5, \end{aligned} \tag{24}$$

$$\begin{aligned} k^{(7)}_{\text{eff},i} = {} & L_i^8 k^{(7)} + 4L_i^9 F_i\left[2k^{(2)}k^{(6)} + 2k^{(3)}k^{(5)} + \left(k^{(4)}\right)^2\right] \\ & + 12\,L_i^{10} F_i^2\left[\left(k^{(3)}\right)^3 + 3\left(k^{(2)}\right)^2 k^{(5)} + 6k^{(2)}k^{(3)}k^{(4)}\right] \\ & + 60L_i^{11} F_i^3\left(k^{(2)}\right)^2\left[2k^{(2)}k^{(4)} + 3\left(k^{(3)}\right)^2\right] \\ & + 330L_i^{12} F_i^4\left(k^{(2)}\right)^4 k^{(3)} + 132L_i^{13} F_i^5\left(k^{(2)}\right)^6, \end{aligned} \tag{25}$$

where

$$F_i = f^{(N-1)}_{zz\,|i}\frac{k^{(1)}}{v}. \tag{26}$$

All lower-order terms (the permanent dipole moment is assumed to be zero) in the nonlinear polarization series contribute to the higher-order hyperpolarizabilities in Eqs. (20)-(25). The cascading contributions are ordered in terms of powers of F_i. For example, the mixing of two lower-order responses results in a higher-order

response in which the magnitude depends on F_i, while the mixing of three lower-order responses depends on the value of F_i^2.

Note that the dipole approximation may not be sufficient to express the effective response in many molecular systems because additional terms in the multipole expansion may make significant contributions to the effective hyperpolarizabilities. This is apparent, particularly at higher-orders, where, for example, the last term in Eq. (25) is a fifth-order cascading contribution.

III. APPLICATIONS TO SINGLE-COMPONENT SYSTEMS

A. Bound and strained systems

Among the geometric quantities affecting the susceptibility in a lattice with a finite number of atoms/molecules are the shape of the surface that contains the lattice, the shape of a primitive cell, and the beam (applied field) profile. Previous investigations for a top hat beam through a thin film [10] show enhancements due to cascading when a system is sharply bounded along the beam direction. The shape of the primitive cell is known to dramatically change the local field in strained crystal lattices as well.[21]

There are many models that assume a potential from permanent dipoles on an infinite Bravais lattice for approximating macroscopic systems,[22–25] but we wish to approach the boundary problem via field-matter interactions, beginning with the perfect dipole approximation at each point on a finite lattice. This method requires knowledge about the entire system and all boundary locations, and thus is more computationally expensive when calculating large systems. The formalism discussed in this section is well suited for modeling cascaded nonlinearities through molecular interactions near interfaces. This method of summing dipole fields does not diverge anywhere on the lattice. Our method's utility is that it approximates the nonlinear optical cascading contributions in a finite system without any assumptions as to the linear/nonlinear behavior of the macroscopic field.

In addition to adjusting boundaries of a lattice we can also strain the lattice to change the cascaded nonlinear response of the system. Taking a large system of molecules on a tetragonal lattice with constants $\{a,a,c\}$, the zz-component of the geometric factor, $f_{zz\,|i}^{(N-1)}$, monotonically increases as c/a decreases. Figure 1(a) shows how the z-component scales as a function of c/a for a molecule located in the center of a large sphere constructed from tetragonal primitive cells.

As anticipated, the dimensionless geometric factor, $f_{zz\,|i}^{(N-1)}$, rapidly decreases and becomes negative as c/a is increased due to the influence of all other molecules. In contrast, $f_{zz\,|i}^{(N-1)}$ rapidly becomes large as c/a falls below unity. Also, a defining feature of the calculation appears

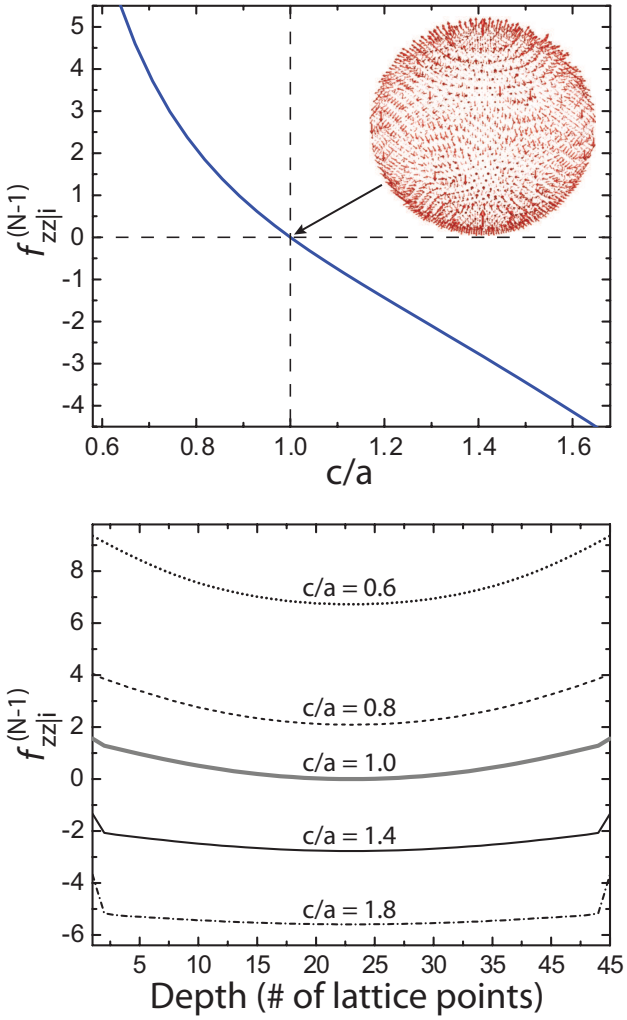

FIG. 1. (a) A graph of first-order correction to $f_{zz\,|i}^{(N-1)}$ for a molecule at the center of a sphere plotted as a function of the lattice vector in the direction of the applied field, c, divided by a lattice vector perpendicular to the field, a. The inset shows a sphere constructed from a cubic lattice where molecules near the surface have a nonzero $f_{\alpha z\,|i}^{(N-1)}$ due to surface roughness. (b) The zz-component of the first-order approximation to the geometric factor, $f_{zz\,|i}^{(N-1)}$, as a function of depth through the center of a strained $45 \times 45 \times 45$ cubic lattice, where we have probed through a surface with zero electric flux and travel normally between the interfacial boundaries.

when $c = a$, where all cascading fields for this center molecule cancel, *i.e.*, $F_i = 0$. Thus, for large cascading enhancements (large $f_{zz\,|i}^{(N-1)}$), one would prefer aligned disk-like molecules with the applied field oriented along the short molecular axis as opposed to rod-like molecules with the applied field oriented along the long molecular axis.

By considering both the microscopic structure and the macroscopic geometry, we can further increase F_i for systems of molecules with constant v. Figure 1(b) shows how $f_{zz\,|i}^{(N-1)}$ varies between two transverse interfa-

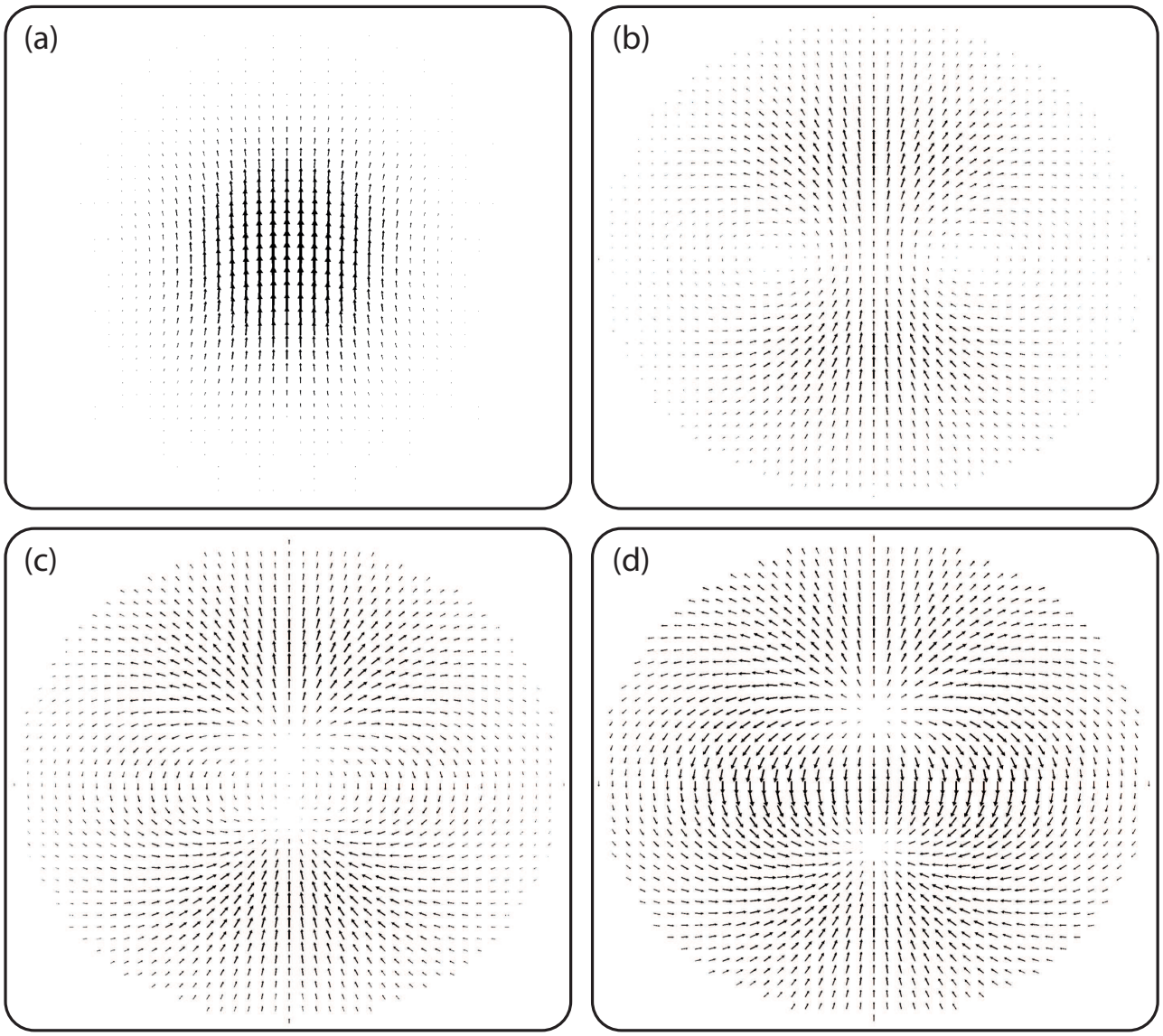

FIG. 2. A vector diagram of the first-order correction to the linear dipole fields for the center layer of a thin film subject to a Gaussian beam. The film thicknesses are (a) 1 layer, (b) 7 layers, (c) 15 layers, and (d) 55 layers of a cubic lattice system with side lengths that extend far beyond the edge of the graphic.

cial boundaries in a strained $45 \times 45 \times 45$ cube with a tetragonal lattice structure. Note that at the boundary locations, even in a highly-elongated tetragonal lattice, $f_{zz\,|i}^{(N-1)}$ is much larger than the next calculated interior-location. This result illustrates the ability of a thin film to enhance the effects of cascading.

B. Dipolar electric field distributions

In this section we examine fixed lattices subject to an optical beam profile that is smaller than the transverse size of the system. An example would be that of the previously studied top hat beam,[10] where the molecules both inside and outside the beam are optically relevant. Here, we focus our attention on a long-wavelength monochromatic beam with a Gaussian profile.

Figure 2 shows four vector diagrams that illustrate the directional components of the field due to the polarization of other molecules in the system. The unit cells are cubic and the size of the arrows are relative to each other in all parts (a)-(d), where we have arbitrarily scaled the maximum value of the dipole field. In these diagrams, we plot only the first-order iterative correction due to linear dipoles that are subject to a vertically polarized applied field. The diagrams show the induced field at the center layer of a thin film subject to a Gaussian beam, where we have truncated the illustrations beyond the edge of the beam waist (where the electric field falls below $1/e$

of the peak value). (We assume that the beam is unchanged during transport through the film's thickness, but we expect that the longitudinal propagation through thick films will be affected by the assumed nonlinear index via the well-known self-focusing phenomenon and the inhomogeneous cascading predicted by $f^{(N-1)}_{\alpha z\,|i}$.)

As shown in the progression from Fig. 2(a)-(d), the competition between the in-plane and out-of-plane polarizations contribute to the electric field in the middle layer in nontrivial ways. For samples thicker than 55-layers, there is little change in the field profile at the center layer for these lattice/beam parameters. The topology of the field profile due to the other dipoles at the center layer, and in the scaling limit, depends on the ratio of the beam diameter to the propagation length.

Topological considerations are useful for understanding the successive frames as one adds layers, where we adjoin a "neighborhood at infinity" to make each of these a map of a vector field on a spherical surface, S^2. If we imagine the vector field over the sphere, there are two zeros of the vector fields in each panel of Fig. 2. The line integrals of the vector fields around regions containing the zeros in Figs. 2(a) and 2(b) have matched positive and negative vorticity. On the other hand, the line integrals of the Hodge dual vector field on those two diagrams are zero.[26] The opposite is true for Figs. 2(c) and 2(d), where the line integrals of the Hodge dual to this vector field (essentially the integral over the divergence of the original vector field) give positive and negative vorticity around the zeros of the field at these locations. Indeed, Figs. 2(b) and 2(d) possess the same topological features as each other's Hodge duals just as vortices and sources are Hodge duals. In this vein, a diagram of the center layer for an 11-layer thick material (between Figs. 2(b) and 2(c)) is nearly self-dual.

Ultimately, the form of Fig. 2(d) is the asymptotic form expected from the polarization of the other layers. Figure 2(a) is as expected from no contributing polarization in the other layers. Thus, these topological considerations support the logical progression found by the simulations.

C. Real systems: monolayers of close-packed C_{60}

We now focus our attention on monolayers of close-packed C_{60} in different lattice structures illuminated by a coherent beam. Our test molecule is chosen to be C_{60} fullerene, which is known for its large third-order susceptibility. Because there are larger cascading enhancements at higher concentration, we consider a hexagonal close-packed structure for this study. Monolayers of C_{60} form hexagonal lattice structures at room temperature, where the distance of separation between the centers of mass between nearest neighbors is approximately $10.04\mathring{A}$.[27] As a comparative study, we look at the vertical and horizontal orientations of the lattice as well as a honeycomb structure. The off-resonant beam carrying the applied field is propagating in the x-direction and vertically polarized in the z-direction. The diameter of the Gaussian beam is 150 nm, where the location of the electric field is $1/e$ of its peak value (intensity is $1/e^2$ of its peak value). The calculated region for all contributions of molecular interactions has a diameter of 180 nm, where the average effective susceptibilities are calculated within the beam waist after all contributions from the extended region outside the beam waist have been taken into account.

Due to the large intrinsic values of the odd-ordered susceptibilities of C_{60}, the polarizability and second hyperpolarizability are estimated by the three level ansatz.[28–30] The values for the oscillator strengths and their corresponding transition energies were previously reported by Leach, *et al.*[31, 32] Truncating the series in the perturbation solution for the (hyper)polarizabilities to only three states gives $k^{(1)} = 1.85 \times 10^{-23}\mathrm{cm}^3$ and $k^{(3)} = 3.41\times10^{-35}\mathrm{erg}^{-1}\mathrm{cm}^5$.[10] Also, $k^{(0)} \approx 0$, $k^{(2)} \approx 0$, and $k^{(4)} \approx 0$ due to the near spherical symmetry of C_{60}. Note that using the standard time-dependent perturbation approach,[33] truncation to a three level model may greatly overestimate the higher-order polarizabilities. We only compute the cascaded contribution to the fifth-order susceptibility and ignore the direct $k^{(5)}$ contribution. The peak applied electric field used to calculate the values given in Table I is 10^6 StatV/cm, which allows for non-negligible contributions from both the polarizability and second hyperpolarizability.

We consider only the scalar (hyper)polarizabilities, though small values of $p_{y\,|i}$ will be present. We approximate the cascading contribution using the scalar values, and we calculate out to a third-order iteration (as explained in the Appendix). The average effective fifth-order susceptibility (susceptibility defined by the applied field with local field and cascading enhancements) for the region inside the beam waist can be approximated by

$$\left\langle \chi^{(5)} \right\rangle^{[n]} = \frac{k^{(5)}}{V} \sum_i^N \left(L_i^{[n]} \right)^6 + \left\langle \chi^{(5)}_{\mathrm{casc}} \right\rangle^{[n]} \tag{27}$$

where

$$\left\langle \chi^{(5)}_{\mathrm{casc}} \right\rangle^{[n]} = 3N \left(\frac{k^{(3)}}{V} \right)^2 \sum_i^N \left(L_i^{[n]} \right)^7 \left(f_i^{(N-1)} \right)^{[n]}. \tag{28}$$

Here, we denote the total volume by $V = Nv$ and the nth-order iterative correction by the superscript $^{[n]}$ as discussed in Section II and the Appendix. The average fifth-order susceptibility $\left\langle \chi^{(5)}_{\mathrm{casc}} \right\rangle$ is calculated from an arithmetic average of the microscopic response. Table I lists values of $\left\langle \chi^{(5)}_{\mathrm{casc}} \right\rangle$ for the vertical and horizontal lattice alignments of hexagonal and honeycomb monolayers subject to a Gaussian beam. The values of $\left\langle \chi^{(5)}_{\mathrm{casc}} \right\rangle^{[n]}$ for

TABLE I. Monolayers of C_{60} subject to a vertically polarized Gaussian beam. $\left\langle \chi^{(5)}_{\text{casc}} \right\rangle$ values are $\times 10^{-26}\text{cm}^4\text{erg}^{-2}$.

Lattice type	Vertical hexagonal	Horizontal hexagonal	Vertical honeycomb	Horizontal honeycomb
Diagram	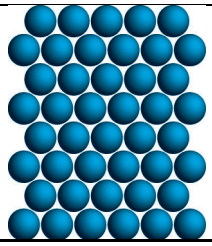	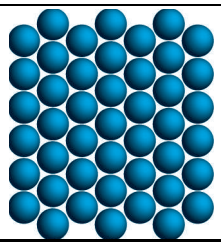	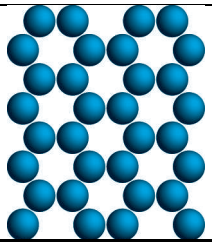	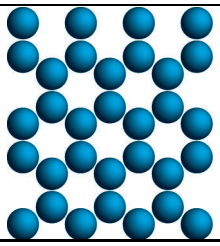
$\left\langle \chi^{(5)}_{\text{casc}} \right\rangle^{[3]}$	4.34	4.34	1.91	1.91
$\left\langle \lvert p_y \rvert^{[1]} \right\rangle$ / $\left\langle \lvert p_z \rvert^{[1]} \right\rangle$	0.0058	0.0006	0.0011	0.0006

The difference between the response in a hexagonal and honeycomb lattice can be understood by using a 2/3 fill factor in Eq. (28). The lattice geometry and nearest neighbor distance remain the same, but the concentration has been reduced by the fill factor, and therefore, we find that the computed honeycomb response is roughly 4/9 that of the computed hexagonal lattice, confirming the greater significance of cascading in the filled, close-packed, structure.

a Gaussian and top hat beam are similar even though the Gaussian beam has a smaller applied field at all molecules except at the center, when the peak value is equal to that of the top hat beam. This can be understood by the on-average increase of $\mathcal{P}_{i,j}$ as we move further from the center of the Gaussian beam. Note that although the responses between the two types of beam profiles are the same, the magnitude of the cascading contribution for a Gaussian beam (with the peak value equal to that of the top hat beam's) is smaller than that resulting from a top hat beam because the susceptibility is multiplied by the tapered Gaussian beam's applied field. Rotating the polarization of a linearly polarized beam between the vertical and horizontal lattice alignments also shows negligible changes in the cascading contribution for both the hexagonal and honeycomb monolayers.

For the hexagonal monolayer subject to a Gaussian beam profile, the values from the first and second iteration change by $< 3\%$. Thus, a first-order approximation to the iterative method is fairly accurate in this scenario and does not carry the computational expense of higher orders that require interactions between polarization directions via tensor components. The iterative method converges quickly, typically changing only in the fifth digit from the second to the third iteration for these monolayers. All iterations after the second (tested out to 20 iterations for stability purposes) showed a stable precision much greater than the uncertainties of the model due to the model's approximations, such as point dipoles, truncated eigenstates, and nearest-neighbor distances.

Again, note that a scalar approximation is also used to generate the values in Table I. In the bottom row, we compare the average dipole moment in the horizontal direction to the dipole moment in the direction parallel to the applied field. The dipole moment ratio never exceeds 0.6% during the iterations, and thus, further justifies the approximation of a scalar response.

IV. APPROXIMATING CASCADING IN POLED GUEST-HOST SYSTEMS

So far we have only considered systems with a single species of atom/molecule. The lattice model, however, can be further generalized to include several molecules with different optical properties. A dipole moment can then be written for individual molecules, where the dependencies on all fields are taken into account including the field contributions from the other species.

To illustrate the inclusion of more than one type of atom or molecule, we choose a dye-doped polymer system. The two main advantages of placing active nonlinear molecules in a polymer are (1) the large linear susceptibilities of many polymers that increase the local field and (2) the ability to align the nonlinear dopant in the medium.[34–36] We use the lattice approximation to model the field enhancement via a randomized occupation of the lattice sites by the guest species. A host cluster is approximated as a point dipole at each occupied lattice site, which we call the host cluster dipole approximation for nonconjugated polymers. Although we take the guest species to be uniaxially aligned molecules and use a lattice approximation, these simplifications may be removed for a more general result.

We assume that all dopant molecules in the system have (hyper)polarizabilities in the $\hat{z}$-direction that are equal to the orientational averaged (hyper)polarizabilities and all other components are negligible, *e.g.*, $\left\langle k^{(2)} \right\rangle = \left\langle k^{(2)}_{zzz} \right\rangle = \left\langle \cos^3\theta \right\rangle k^{(2)}_{zzz}$ and $\left\langle k^{(2)}_{ijk} \right\rangle \approx 0$ for all cases other than $i = j = k = z$. This approxi-

mation is valid for one-dimensional molecules oriented at small angles from the direction of the electric field, where $\left\langle k^{(2)}_{zxx}\right\rangle = \left\langle k^{(2)}_{xzx}\right\rangle = \left\langle k^{(2)}_{xxz}\right\rangle = \left\langle \cos\theta \sin^2\theta\right\rangle k^{(2)}_{zzz}/2$, which is small due to the $\sin^2\theta$ contribution.[37, 38] A full treatment of the cascading contributions to $k^{(3)}$ for a pair of one-dimensional molecules in an electric field at fixed locations is given in Ref. [18]. For our current example, however, we ignore the azimuthal angle and treat only the average polar angle in an attempt to reduce orientational complexities. Therefore, for fixed molecules, we define

$$\kappa^{(n)} = \left\langle \cos^{n+1}(\theta)\right\rangle k^{(n)}, \tag{29}$$

where all other tensor components are assumed negligible for small angles.

We define p^A as the dipole moment of the linear host species and p^B as the dipole moment of the guest species. The two dipole moment equations are

$$p^A_i = \kappa^{(1)}_A \left(E^a_i + \sum_{j\neq i}^{N_A-1} h_{i,j}\frac{p^A_j}{v} + \sum_j^{N_B} f_{i,j}\frac{p^B_j}{v}\right), \tag{30}$$

$$p^B_i = \sum_n \kappa^{(n)}_B \left(E^a_i + \sum_j^{N_A} h_{i,j}\frac{p^A_j}{v} + \sum_{j\neq i}^{N_B-1} f_{i,j}\frac{p^B_j}{v}\right)^n \tag{31}$$

where $h_{i,j}$ and $f_{i,j}$ are the geometry-dependent factors (to a first-order approximation using the iterative method) for species A and B that account for a dipole field from all j molecules. We treat $h_{i,j}$ and $f_{i,j}$ as scalars because we choose our uniaxial molecules to be aligned with the applied field polarization. Note that for higher-order iterative corrections, we would keep track of each host molecule's $\left(\kappa^{(1)}_{A\,|i}\right)^{[m]}$ and guest molecule's $\left(\kappa^{(n)}_{B\,|i}\right)^{[m]}$.

Because we are interested in the nonlinear response of guest species, we first solve Eq. (30), which gives

$$p^A_i = \kappa^{(1)}_A \mathcal{L}^A_i \left(E^a_i + \sum_j^{N_B} f_{i,j}\frac{p^B_j}{v}\right), \tag{32}$$

where

$$\mathcal{L}^A_i = \left(1 - \sum_{j\neq i}^{N_A-1} h_{i,j}\mathcal{P}^A_{i,j}\frac{\kappa^{(1)}_A}{v}\right)^{-1}. \tag{33}$$

Here, $\mathcal{L}^A_i$ is the first-order correction to the local field at a host cluster due to all other host clusters, where we have also included the scaling factor $\mathcal{P}^A_{i,j} = p^A_j/p^A_i$ for molecules subject to a spatially varying applied field with the same approximations described in Section II.

Substituting Eq. (32) into Eq. (31) gives

$$p^B_i = \sum_n \kappa^{(n)}_B \left[(1+\mathcal{Q}_i)\, E^a_i + \left(\mathcal{S}_i + f^{(N_B-1)}_i\right)\frac{p^B_i}{v}\right]^n \tag{34}$$

where

$$\mathcal{Q}_i = \frac{\kappa^{(1)}_A}{v}\sum_j^{N_A} h_{i,j}\mathcal{L}^A_j\mathcal{E}_{i,j}, \tag{35}$$

$$\mathcal{S}_i = \frac{\kappa^{(1)}_A}{v}\sum_j^{N_A} h_{i,j}\mathcal{L}^A_j\sum_k^{N_B} f_{j,k}\mathcal{P}^B_{i,k}, \tag{36}$$

and

$$f^{(N_B-1)}_i = \sum_{j\neq i}^{N_B-1} f_{i,j}\mathcal{P}^B_{i,j}. \tag{37}$$

The last term in Eq. (35) allows for a spatially varying applied field, where

$$\mathcal{E}_{i,j} = \frac{E^a_j}{E^a_i}. \tag{38}$$

Solving Eq. (34) self-consistently and substituting into Eq. (16) gives the (hyper)polarizabilities of guest molecules. Off-resonance, the first-order contributions to the effective polarizability, hyperpolarizability, and second hyperpolarizability of the ith guest molecule are

$$\kappa^{(1)}_{\mathrm{eff},B,i} = \kappa^{(1)}_B \frac{1+\mathcal{Q}_i}{1-\left(f^{(N_B-1)}_i + \mathcal{S}_i\right)\frac{\kappa^{(1)}_B}{v}}, \tag{39}$$

$$\kappa^{(2)}_{\mathrm{eff},B,i} = \kappa^{(2)}_B \frac{(1+\mathcal{Q}_i)^2}{\left(1-\left(f^{(N_B-1)}_i + \mathcal{S}_i\right)\frac{\kappa^{(1)}_B}{v}\right)^3}, \tag{40}$$

and

$$\kappa^{(3)}_{\mathrm{eff},B,i} = \frac{\kappa^{(3)}_B (1+\mathcal{Q}_i)^3}{\left(1-\left(f^{(N_B-1)}_i + \mathcal{S}_i\right)\frac{\kappa^{(1)}_B}{v}\right)^4} + \frac{2}{v}\left(\kappa^{(2)}_B\right)^2 \frac{(1+\mathcal{Q}_i)^3\left(f^{(N_B-1)}_i + \mathcal{S}_i\right)}{\left(1-\left(f^{(N_B-1)}_i + \mathcal{S}_i\right)\frac{\kappa^{(1)}_B}{v}\right)^5}. \tag{41}$$

Equations (39)-(41) are similar in form to Eqs. (17), (20), and (21) except for the terms $\mathcal{Q}_i$ and $\mathcal{S}_i$. The first additional term, $\mathcal{Q}_i$, comes from the self-consistent linear field correction to the guest molecules from the surrounding host material. The second additional term, $\mathcal{S}_i$, is similar to a second-order iterative correction in the single species model, where a nonlinear process from a guest molecule alters the field that a host cluster experiences (including the modified field corrections from the host), which in turn affects the field at any guest molecule.

As an example, we consider a *thin, poled, guest-host film of disperse orange 3 (DO3) molecules dissolved in poly(methyl methacrylate) (PMMA).* DO3 is

an azobenzene dye with a molecular weight of approximately 242 g/mol. PMMA has a density of 1.12 g/cm^3, and setting the cubic lattice constant to approximately 7.11 Å(the volume of a cubic cell is 3.19×10^{-22} cm^3) gives an effective molecular weight of the host cluster to be that of DO3 (not the actual molecular weight of a host molecule). For PMMA with a dielectric constant, ϵ_r, of 2.85, we find a host cluster polarizability of approximately 3.27×10^{-23} cm^3 in Gaussian units via the Clausius-Mossotti equation for an isotropic bulk material,

$$k_A^{(1)} = \frac{3V}{4\pi N}\left(\frac{\epsilon_r - 1}{\epsilon_r + 2}\right), \tag{42}$$

where V is the total volume given in units of cm^3, N is the the number of host clusters, and the presence of 4π in the denominator (lack of ϵ_0 in the numerator) converts the polarizability to Gaussian units. Note that $k_A^{(1)}$ is assumed to be isotropic, and therefore, $\kappa_A^{(1)} = k_A^{(1)}$. The guest molecules are assumed to be at a concentration of 1.56%, which roughly corresponds to one guest molecule per every 64 lattice sites. We consider a sample of thickness 9.24 nm (13 lattice sites thick), subject to a Gaussian beam with a diameter of approximately 150 nm (roughly 211 lattice sites).

The guest molecules are assumed mostly aligned, with an average polar angle, $\langle\theta\rangle = 15°$, from the $\hat{z}$-direction (direction of the polarized light). The real off-resonant value for the polarizability was evaluated using the ORCA program system [39] and was 7.99×10^{-23} cm^3. To optimize the molecular structure prior to approximating the polarizability, geometry relaxation steps were taken after every energy calculation using the BP functional in conjunction with the TZV basis set.[40–42] The hyperpolarizability and second hyperpolarizability of DO3 have been tabulated as 2.77×10^{-29} erg$^{-1/2}$cm^4 and 2.56×10^{-34} erg^{-1}cm^5, respectively.[43, 44] The corresponding orientational averaged values at 15° are then $\kappa_B^{(1)} = 7.45 \times 10^{-23}$ cm^3, $\kappa_B^{(2)} = 2.50 \times 10^{-29}$ erg$^{-1/2}$cm^4, and $\kappa_B^{(3)} = 2.23 \times 10^{-34}$ erg^{-1}cm^5.

The average of the first-order iterative cascaded contribution to the orientationally averaged, scalar, second hyperpolarizability, $\left\langle \kappa_{\text{eff}}^{(3)} \right\rangle$, was calculated to be 2.77×10^{-33} erg^{-1}cm^5, where the first term in Eq. (41) is 2.61×10^{-33} erg^{-1}cm^5 and the second term in Eq. (41) is 1.61×10^{-34} erg^{-1}cm^5. The average third-order susceptibility as a function of the applied field (assuming the off-resonant nonlinear contribution to the susceptibility of PMMA is negligible), $\left\langle \chi_{\text{eff}}^{(3)} \right\rangle$, is 1.20×10^{-13} erg^{-1}cm^2. For comparative purposes, if we were to remove the PMMA and observe the DO3 in a gas phase while keeping the long molecular axis aligned with the field making an average polar angle of 15°, we calculate the orientationally averaged third-order susceptibility $\left\langle \chi_{\text{eff}}^{(3)} \right\rangle_{\text{gas-orient}} \approx N_B \kappa^{(3)}/V$ to be 9.69×10^{-15} erg^{-1}cm^2. Thus, the presence of the linear host greatly enhances the nonlinear susceptibility of the system due to both local field and cascading effects.

When modeling guest-host systems, the $\mathcal{Q}_i$'s depend on the details of the microscopic configuration. Note that these $\mathcal{Q}_i$'s, which refer to the host's linear modification to the applied field, can be both positive and negative. Thus, our approach allows one to calculate the cascaded contribution *ab initio* for a nano-engineered system with a specific geometry.

V. CONCLUSIONS

We used a self-consistent method to derive the scalar effective nonlinear susceptibilities of bounded systems out to seventh-order. The lattice model allows for fast calculations of geometric factors that epitomize the electronic interactions between polarizable atoms and molecules. By substituting these geometric factors into the calculation for the response of a system of dipoles, we have shown that boundary effects and deviations from a cubic lattice may enhance the local field and cascading contributions to the off-resonant optical responses. The resultant field due to dipoles induced by a Gaussian beam has been characterized for different film thicknesses. We also applied our cascading approach to calculate the nonlinear cascaded contribution to the fifth-order susceptibility in monolayers of C_{60}.

We further developed this approach in application to a guest-host model, where a linear-optical host is doped with nonlinear-optical molecules. By limiting the study to fixed molecules, we derive expressions for the effective, nonlinear responses of the guest molecules that include all linear- and nonlinear-optical cascading configurations. We used a DO3-doped PMMA system (1.56% DO3) as an example in which we show more than an order-of-magnitude increase in the third-order susceptibility with respect to an oriented gas state (no host present).

This work may lead to new approaches for calculating additional self-focusing phenomena in beam stability simulations, which may impact optical limiter designs and other nonlinear devices.

ACKNOWLEDGMENTS

The authors are grateful to the National Science Foundation for financial support from the Science and Technology Center for Layered Polymeric Systems under grant number DMR 0423914. The authors are also grateful for the support of the Department of Development, State of Ohio, the Chancellor of the Board of Regents, State of Ohio, and the Third Frontier Commission, which provided funding in support of the Research Cluster on Surfaces in Advanced Materials.

APPENDIX A: HIGHER-ORDER CORRECTIONS AND THE ITERATIVE PROCESS

For many systems, Eq. (11) may not give a close enough approximation to the effective (hyper)polarizabilities. In these cases, further iterations to the self-consistent dipole equation are necessary to give a more accurate description of the off-resonant cascading contribution. For the first order correction, we obtained solutions in terms of $f^{(N-1)}_{\alpha\beta\,|i}$. The iterative method is described following Eq. (8), and for the second-order correction, gives

$$\begin{aligned} p^{[2]}_{\alpha\,|i} = {} & k^{(0)}_{\alpha\,|i} + k^{(1)}_{\alpha\beta\,|i}\left(E^a_{\beta\,|i} + \sum_{j\neq i}^{N-1} g_{\beta\gamma\,|i,j}\mathcal{P}^{[1]}_{\gamma\,|i,j}\frac{p^{[2]}_{\gamma\,|i}}{v_c}\right) \\ & + k^{(2)}_{\alpha\beta\mu\,|i}\left(E^a_{\beta\,|i} + \sum_{j\neq i}^{N-1} g_{\beta\gamma\,|i,j}\mathcal{P}^{[1]}_{\gamma\,|i,j}\frac{p^{[2]}_{\gamma\,|i}}{v_c}\right) \\ & \times\left(E^a_{\mu\,|i} + \sum_{j\neq i}^{N-1} g_{\mu\gamma\,|i,j}\mathcal{P}^{[1]}_{\gamma\,|i,j}\frac{p^{[2]}_{\gamma\,|i}}{v_c}\right) + \cdots, \end{aligned} \tag{A1}$$

The effective (hyper)polarizabilities given in Eqs. (17) and (20)-(25) are first-order corrections to the response of molecules that are polarized along the direction of the applied field. With a more rigorous approach, one can find the effective (hyper)polarizabilities for all possible components. Thus, we can define $\mathcal{P}^{[1]}_{\alpha\,|i,j}$ in terms of these first-order effective (hyper)polarizabilities and the applied electric field,

$$\mathcal{P}^{[1]}_{\alpha\,|i,j} = \frac{\sum_n \left(k^{(n)}_{\alpha\beta\mu\nu\cdots\,|j}\right)^{[1]} E^a_{\beta\,|j}E^a_{\mu\,|j}E^a_{\nu\,|j}\cdots}{\sum_n \left(k^{(n)}_{\alpha\beta\mu\nu\cdots\,|i}\right)^{[1]} E^a_{\beta\,|i}E^a_{\mu\,|i}E^a_{\nu\,|i}\cdots}, \tag{A2}$$

where we have altered the notation of the effective (hyper)polarizabilities to account for higher-order corrections, *i.e.*, k_{eff} in Section II is the first-order correction in the iterative method $k^{[1]}$.

For a known spatial distribution of the applied electric field, Eq. (A2) has some specified value for each component of a molecule i with respect to some other molecule j, which is similar to that used for the updates in Ref. [45]. Once the single molecule (hyper)polarizabilities have been inserted into the first-order correction to the effective (hyper)polarizabilities, the first-order corrected effective (hyper)polarizabilities are inserted into Eq. (A2). Then, we define

$$\left(f^{(N-1)}_{\alpha\beta\,|i}\right)^{[1]} = \sum_{j\neq i}^{N-1} g_{\alpha\beta\,|i,j}\mathcal{P}^{[1]}_{\beta\,|i,j}, \tag{A3}$$

where $\left(f^{(N-1)}_{\alpha\beta\,|i}\right)^{[0]}$ is given in Eq. (11).

To find the second correction to the off-resonant (hyper)polarizabilities for the ith molecule, we substitute Eq. (11) into Eq. (A1), and then substitute the resultant equation into

$$\left(k^{(n)}_{\alpha\beta\mu\nu\cdots\,|i}\right)^{[2]} = \frac{1}{n!}\frac{\partial^n p^{[2]}_{\alpha\,|i}}{\partial E^a_{\alpha\,|i}\partial E^a_{\beta\,|i}\partial E^a_{\mu\,|i}\partial E^a_{\nu\,|i}\cdots}\bigg|_{\boldsymbol{E}^a=0}. \tag{A4}$$

These values are the second-order corrections to the (hyper)polarizabilities. This simple step-by-step iterative process may be used to evaluate these higher-order corrections, where a loop may be implemented until the effective hyperpolarizabilities converge. Third order-corrections are found via the next iteration, where we replace the superscripts [2] by the superscripts [3] and use values obtained in from the second-order corrections by replacing the superscripts [1] by the superscripts [2]. Following this same principle, higher-order iterative approximations can be obtained.

[1] J. H. Andrews, K. L. Kowalski, and K. D. Singer, Phys. Rev. A **46**, 4172 (1992).
[2] G. I. Stegeman, M. Sheikbahae, E. W. Van Stryland, and G. Assanto, Opt. Lett. **18**, 13 (1993).
[3] G. I. Stegeman, D. J. Hagan, and L. Torner, Opt. and Quant. Electron. **28**, 1691 (1996).
[4] A. Baev, J. Autschbach, R. W. Boyd, and P. N. P., Opt. Ex **18**, 8713 (2010).
[5] K. Dolgaleva, R. W. Boyd, and J. E. Sipe, Phys. Rev. A **76**, 063806 (2007).
[6] K. Dolgaleva, H. Shin, and R. W. Boyd, Phys. Rev. Lett. **103**, 113902 (2009).
[7] K. Dolgaleva, H. Shin, R. Boyd, and J. Sipe, in *Lasers and Electro-Optics, 2009 and 2009 Conference on Quantum electronics and Laser Science Conference* (2009) pp. 1–2.
[8] K. Dolgaleva and R. W. Boyd, Adv. Opt. Photon. **4**, 1 (2012).
[9] N. J. Dawson, B. R. Anderson, J. L. Schei, and M. G. Kuzyk, Phys. Rev. A **84**, 043406 (2011).
[10] N. J. Dawson and J. H. Andrews, J. Phys. B **45**, 035401 (2012); Corrigendum, *ibid.* **45**, 229501 (2012).
[11] N. Bloembergen, *Nonlinear Optics*, 4th ed. (World Scientific, Singapore, 1996).
[12] A. Moroz, J. Opt. Soc. Am. B **26**, 517 (2009).
[13] M. E. Crenshaw, Phys. Rev. A **78**, 053827 (2008).
[14] P. C. Ray and J. Leszczynski, Chem. Phys. Lett. **399**, 162 (2004).
[15] P. A. Lebwohl and G. Lasher, Phys. Rev. A **6**, 426 (1972).
[16] N. V. Priezjev and R. A. Pelcovits, Phys. Rev. E **63**, 062702 (2001).
[17] S. Romano, Int. J. Mod. Phys. B **16**, 2901 (2002).

[18] N. J. Dawson, B. R. Anderson, J. L. Schei, and M. G. Kuzyk, Phys Rev. A **84**, 043407 (2011).

[19] G. Asanto, D. Neher, G. I. Stegeman, W. E. Torruellas, M. B. Marques, W. H. G. Horsthuis, and G. R. Möhlmann, Mol. Cryst. Liq. Cryst. **222**, 33 (1992).

[20] K. Dolgaleva, H. Shin, R. Boyd, and J. Sipe, in *International Conference on Quantum Information* (Optical Society of America, 2008) p. JMB47.

[21] K. F. Herzfeld, J. Opt. Soc. Am. **17**, 26 (1928).

[22] H. Mueller, Phys. Rev. **47**, 947 (1935).

[23] M. Born and K. Huang, *Dynamical Theory of Crystal Lattices*, The International Series of Monographs on Physics (Oxford University Press, London, 1954).

[24] P. P. Ewald, *Dissertation*, Ph.D. thesis, Ludwig Maximilians University of Munich (1912).

[25] P. P. Ewald, Ann. Phys. **54**, 519 (1917).

[26] S. L. Goldberg, *Curvature and Homology* (Dover, New York, 1962).

[27] J. K. Gimzewski, S. Modesti, T. David, and R. R. Schlittler, J. Vac. Sci. Technol. B **12**, 1942 (1994).

[28] M. G. Kuzyk, Phys. Rev. A. **72**, 053819 (2005).

[29] M. G. Kuzyk, J. Nonl. Opt. Phys. & Mat. **15**, 77 (2006).

[30] J. Pérez-Moreno, K. Clays, and M. G. Kuzyk, J. Chem. Phys. **128**, 084109 (2008).

[31] S. Leach, M. Vervloet, A. Desprès, E. Bréheret, J. P. Hare, T. J. Dennis, H. W. Kroto, R. Taylor, and D. R. M. Walton, Chem. Phys. **160**, 451 (1992).

[32] A. Bulgac and N. Ju, Phys. Rev. B. **46**, 4297 (1992).

[33] B. J. Orr and J. F. Ward, Molecular Physics **20**, 513 (1971).

[34] K. D. Singer, M. G. Kuzyk, R. B. Comizzoli, H. E. Katz, M. L. Schilling, J. E. Sohn, and S. J. Lalama, App. Phys. Lett. **53**, 1800 (1988).

[35] M. Eich, A. Sen, H. Looser, G. C. Bjorklund, J. D. Swalen, and R. T. D. Y. Yoon, J. Appl. Phys. **66**, 2559 (1989).

[36] H. L. Hampsch, J. M. Torkelson, S. J. Bethke, and S. G. Grubb, J. Appl. Phys. **67**, 1037 (1990).

[37] T. Rasing, Y. R. Shen, M. W. Kim, J. P. Valint, and J. Bock, Phys. Rev. A **31**, 537 (1985).

[38] M. G. Kuzyk, K. D. Singer, H. E. Zahn, and L. A. King, J. Opt. Soc. Am. B **6**, 742 (1989).

[39] F. Neese, Wiley Interdisciplinary Reviews: Computational Molecular Science **2**, 73 (2012).

[40] J. P. Perdew, Phys. Rev. B **33**, 8822 (1986).

[41] A. D. Becke, Phys. Rev. A **38**, 30983100 (1988).

[42] A. Schaefer, H. Horn, and R. Ahlrichs, J. Chem. Phys. **97**, 2571 (1992).

[43] L. Xiang, Y.-G. Liu, A.-G. Jiang, and D.-Y. Huang, Chem. Phys. Lett. **338**, 167 (2001).

[44] P. Audebert, K. Kamada, K. Matsunaga, and K. Ohta, Chem. Phys. Lett. **367**, 62 (2003).

[45] M. Kühn and H. Kliem, Journal of Physics: Conference Series **142**, 012028 (2008).